

Using new techniques for re-evaluating the physiological ecology of coccolithophores

William M. Balch

Bigelow Laboratory for Ocean Sciences, POB 475, W. Boothbay Harbor, ME 04575, USA. bbalch@bigelow.org

Traditional views of coccolithophore ecology have been firmly rooted in the seminal work of Margalef (1979). He suggested that, within the two dimensional phytoplankton niche space defined by turbulence and nutrients (“Margalef’s Mandala”), coccolithophores fell between the diatoms (which exploit well-mixed, high nutrient regimes) and the dinoflagellates (which exploit stratified, low-nutrient regimes). Margalef’s paradigm extended to growth strategies, too, based on nutrient uptake kinetics. He suggested diatoms to be fast-growing “r” strategists, dinoflagellates to be slower-growing “K” strategists, and coccolithophores to be somewhere between “r” and “K”. Margalef suggested that these functional groups appeared following a mixing event, typically showing succession from the diatom-dominated communities, to coccolithophores, ultimately to dinoflagellates (Fig. 1). It is important to note that other algal groups, such as cyanobacteria, picoeu-

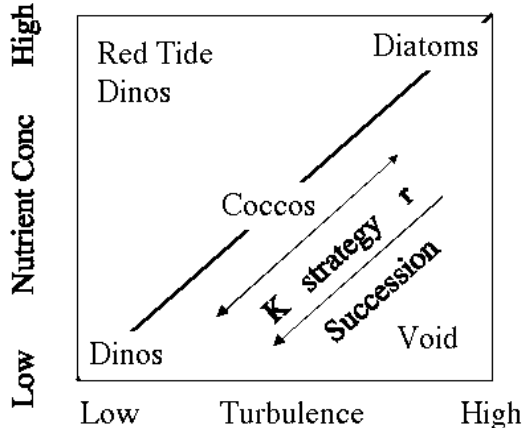


Fig. 1. Re-drawn version of Margalef’s mandala (Margalef 1979) (his fig. 2), illustrating the two-dimensional niche space model of diatoms, dinoflagellates and coccolithophorids relative to turbulence and nutrients.

karyotes, blue-green algae, and prochlorophytes, were not included in the mandala (some of these algal groups were not even known at the time of Margalef's work). Nonetheless, based on the algal classes that he described, we would expect highest coccolithophore abundance, suspended calcite concentration, and calcification in environments of moderate turbulence and nutrients. This paper, although not meant to be an exhaustive review of all coccolithophore ecology, will address the applicability of Margalef's paradigm to some selected recent coccolithophorid observations.

In discussing the niche of coccolithophores relative to diatoms and dinoflagellates, it is important not to overlook some of the details of species distribution described by others. Guillard and Kilham (1977) commented on the importance of cell size in its relation to surface-to-volume ratios and growth rate. They specifically focused on diatoms but their discussion is equally applicable to other algal classes. Moreover, their analysis of the different types of diatoms is somewhat at odds with the Margalef (1979) paradigm since they described specific large diatom species that are more characteristic of oligotrophic, low turbulence environments, as opposed to high turbulence environments. They also highlighted the fact that algal succession can be strongly modulated by grazing pressure. The importance of grazing was also discussed by Margalef (1979).

Similar to the Guillard and Kilham analysis of diatom ecology, Young (1994) defined three ecological communities of coccolithophores, associated with 3 distinct environments: placolith-bearing cells such as *Emiliania huxleyi*, found in coastal or mid-ocean upwelling regions and umbelliform cells such as *Umbellosphaera tenuis*, found in more oligotrophic, nutrient-depleted waters. The last group, floriform cells (such as *Florisphaera profunda*), were associated with deep photic-zone assemblages in low to mid-latitudes. Moreover, Young discussed the appearance of motile cells within the placolith-bearing group; flagellae could substantially enhance the ability of coccolithophores to exploit stratified, nutrient-poor environments. Similar to Margalef's predictions of coccolithophore growth strategies, it is likely that the three groups of coccolithophores defined by Young, show differences in their growth strategies which ultimately would relate to their natural abundance and production of calcium carbonate (otherwise known as particulate inorganic carbon, PIC). Interestingly, it still is not known whether conceptual models such as Young's and Margalef's predict not only coccolithophore abundance in nature, but also their rates of carbon fixation via photosynthesis or calcification. The advent of satellite-based observations of *E. huxleyi* blooms (starting with Holligan et al. (1983)), showed the potential importance coccolithophore calcite to the marine carbon cycle, which subsequently encouraged new research on coccolithophore blooms and calcification rates, under the auspices of the International JGOFS. There has been a profound need to synthesize field observations of coccolithophores in order to link traditional taxonomic enumeration studies to the more process-oriented C studies.

Synthesis of field observations from three oceans

Pacific Ocean (12°N to 12°S along 140°W)

Coccolithophore observations in the Pacific have consisted mostly of microscope enumeration of seawater samples and sediment traps (e.g. (Okada and Honjo 1973, 1975; Okada and McIntyre 1977, 1979; Reid 1980) with considerably less attention devoted to coccolithophore growth and carbon fixation. One study which addressed coccolithophore abundance and their carbon fixation was conducted in the Equatorial Pacific during the summer of 1992, in which stations were run along 140°W, from 12°N to 12°S (Balch and Kilpatrick 1996b). One striking observation from this survey was the confirmation of a dramatic decrease in birefringent detached coccoliths below 60 m depth. Okada and Honjo (Okada and Honjo 1973) also observed decreases in coccolithophore cells as much as 30-40x over the top 200 m in the Equatorial region. Reid (1980) cited significant decreases in the numbers of coccolithophore cells in the North Pacific Gyre, as well. The 1992 study demonstrated a strong association of coccoliths with the Equatorial Current, with lower, but still significant, coccolith concentrations in the South Equatorial Counter Current (SECC) and North Equatorial Counter Current (NECC) (Fig. 2). Okada and Honjo observed a similar enhancement of coccolithophores in the equatorial region between 12°S and 5°N, but their contouring intervals did not allow demarcation of the specific current regimes of the Equatorial Pacific.

Equatorial Pacific patterns of primary production, calcification and calcite standing stock did *not* match the above patterns of the coccolithophore abundance (Balch and Kilpatrick 1996a) (Fig. 3). For example, primary production (performed by coccolithophores and non-coccolithophore algae alike) not surprisingly showed a much broader mesoscale pattern with a maximum near the equator and gradual decreases with increasing latitude. However, calcification rates were more patchy, with a maximum just to the south of, but directly adjoining, the diatom-dominated productivity maximum between the equator and 2°N. This diatom community “outcropped” at the surface at the 2°N convergence front, producing the “Line in the Sea” feature (Archer et al. 1997; Yoder et al. 1994). Directly- adjoining coccolithophore and diatom communities have been observed in other settings and will be discussed more later. The concentration of PIC (comprised mostly of coccolithophores, as opposed to foraminifera and pteropods, due to the small sample volumes) were highest in the Equatorial Pacific, directly under regions of highest calcification (Fig. 3). This suggested the importance of grazing/repackaging of the coccoliths into larger, faster-sinking particles. But the fact that highest PIC concentrations generally did not extend below 100m suggests that some other processes were involved in the removal of the PIC. Given the Equatorial Pacific patterns of calcification, a comparison with total carbon fixation showed that, on an integral basis, coccolithophore calcification represented ~3-12% of the total carbon fixation, with peaks at the equator and in more oligotrophic waters found at latitudes exceeding 7° N or S (see figure 7 of Balch and Kilpatrick (1996b)). Estimates of PIC turnover based on

its standing stock divided by

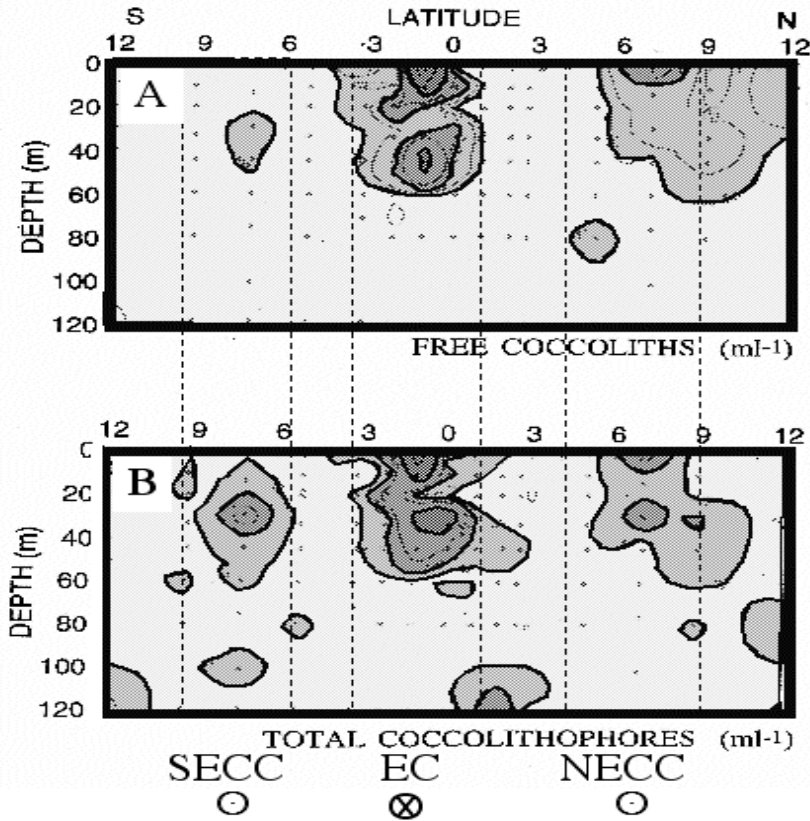


Fig. 2. A) Cross section of coccolith concentration (showing coccoliths detached from coccosphere) across equatorial Pacific Ocean at 140°W from 12°N to 12°S during August and September 1992 (redrawn from fig. 1 of Balch and Kilpatrick (1996b)). Coccolith concentration is designated with darkening shades of gray with the following respective values: $<50\text{ml}^{-1}$ (lightest), $50\text{-}200\text{ mL}^{-1}$, $200\text{-}400\text{ mL}^{-1}$, $>400\text{ mL}^{-1}$ (darkest). B) Section showing concentration of plated coccolithophores along same section in panel A. Coccolithophore concentration is designated with darkening shades of gray with the following respective values: $<5\text{ mL}^{-1}$ (lightest), $5\text{-}9.99\text{ mL}^{-1}$, $10\text{-}40\text{ mL}^{-1}$, and $>40\text{ mL}^{-1}$ (darkest). Re-drawn from figure 2 of Balch and Kilpatrick (1996b)). SECC designates the South Equatorial Counter Current (flowing westward), EC designates the Equatorial Current (flowing eastward), and NECC designates the North Equatorial Counter Current (flowing eastward).

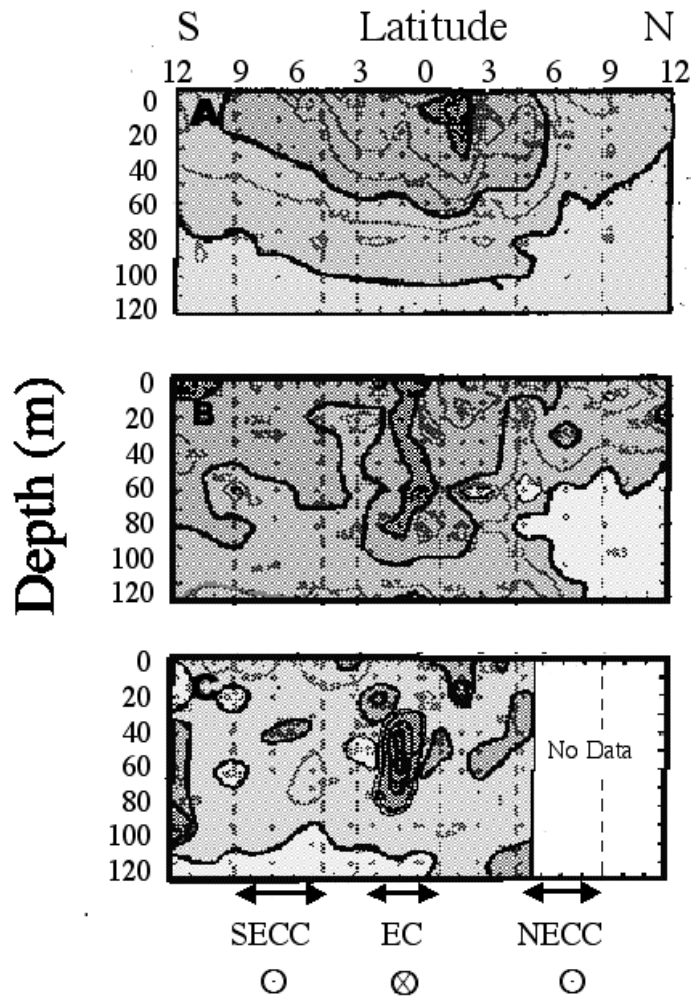


Fig. 3. A) Vertical section of photosynthesis along 140°W (redrawn from fig. 4 of Balch and Kilpatrick (1996b)). Other details of section are as described in Fig. 2. Contour intervals (in units of $\text{mmol organic C m}^{-3} \text{ d}^{-1}$) are designated by progressively-darker gray cross hatching: <0.17 (lightest), 0.17-0.42; 0.43-1.42; >1.42 (darkest). B) Vertical section of calcification along 140°W. Contour intervals (in units of $\mu\text{mol organic C m}^{-3} \text{ d}^{-1}$) are designated by progressively-darker shades of gray: <8.3 (lightest), 8.3-33.3; 33.4-66.7; >66.7 (darkest). C) Vertical section of suspended PIC along 140°W. Contour intervals (in units of $\text{mmol organic C m}^{-3}$) are designated by progressively-darker shades of gray: light <0.17 (lightest), 0.17-0.25; 0.25-0.33; 0.33-1.33; >1.33 (darkest).

its production rate were typically 2-10d. The fact that coccolithophore calcification was highest in Equatorial waters adjoining diatom-dominated communities, certainly is consistent with the Margalef Mandala paradigm, although association of coccolithophores with a region of strong upwelling is not predicted *a priori*. It is important to caution, however, the fact that these Equatorial Pacific calcification data are limited to one season and thus do not allow insight into temporal evolution of the communities.

Another Pacific observation was consistent with predictions based on Margalef's mandala (Margalef 1979). During the 1990's, spectacular coccolithophore blooms were observed in the Bering Sea, previously not seen before in remote sensing images. The blooms generally appeared in late spring/early summer, although turbid water features have been noted in SeaWiFS images as early as February. It now appears that the February events were merely sediment resuspension events over the shallow Continental Shelf region (Broerse et al. 2002). The other mesoscale features in the Bering Sea were indeed coccolithophore blooms, and appeared to be associated with anomalously warm North Pacific conditions (Napp and Hunt 2001) and associated stratification of surface waters.

Indian Ocean (Arabian Sea)

The only parallel measurements of Indian Ocean coccolithophore abundance and calcification are the JGOFS measurements of Balch et al. (2000). The important temporal variable in the northern Indian Ocean is the intense wind forcing associated with the SW Monsoon during the summer and NE Monsoon during the winter (with intervening intermonsoon periods). Abundance of coccolithophores and detached coccoliths (integrated to the base of the euphotic zone) showed 20% higher abundance during the more stratified intermonsoon, but the difference was not significant. Spatially, this translated to highest abundance offshore, with some moderate increases in areas affected by coastal upwelling. In terms of PIC concentrations, there was ~10% more PIC overall during the SW Monsoon, but again, such differences were insignificant. Turnover times of integrated PIC were between 8 and 19d and were not very different from the POC turnover times; this was not expected given the lack of nutritive value in calcite. Unlike cell abundance and PIC, calcification showed a highly significant doubling during the SW monsoon. This raised the interesting possibility that, during the SW monsoon, there was increased calcification in the coastal zone, performed by fewer coccolithophore cells. Indeed, calcification per plated coccolithophore cells was 7x greater during the SW Monsoon, the period of *increased* mixing (Fig. 4). While this analysis incorporated no differences in coccolithophore species composition between the two sampling periods, the observations clearly were not predicted from the Margalef Mandala, *a priori*.

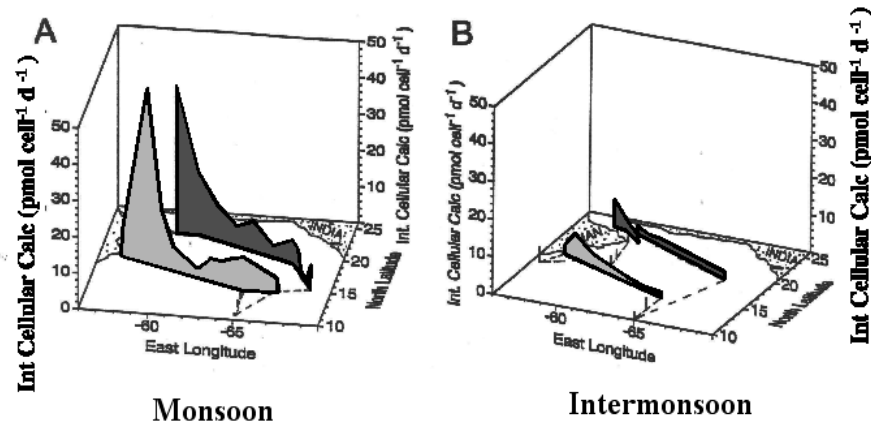


Fig. 4. Integrated calcification per plated coccolithophore cell in the Arabian Sea during A) SW Monsoon and B) Intermonsoon periods (redrawn from Balch (2000)). Northern and southern survey transects are shown in dark gray and light gray, respectively. Cruise mean cellular calcification rate was $17.4 \text{ pmol cell}^{-1} \text{ d}^{-1}$ for the monsoon and $2.5 \text{ pmol cell}^{-1} \text{ d}^{-1}$ for the intermonsoon. They were significantly different with a significance level of $P < 0.05$ (redrawn from Balch et al. (2000)).

Atlantic Ocean

The Atlantic Ocean (including its northern marginal seas) has had some of the most spectacular coccolithophore blooms ever observed, and by far the most measurements of calcification and coccolithophore abundance (Balch et al. 1992; Buitenhuis et al. 1996; Fernández et al. 1993; Garcia-Soto et al. 1995; Holligan et al. 1993; Holligan et al. 1983; Marañón and González 1997; Van der Wal et al. 1995). Observations of coccolithophore calcification in non-bloom situations are not as common (Graziano et al. 2000).

There are a few unifying aspects of North Atlantic coccolithophore bloom observations. Turbid coccolithophore suspensions usually appear during May through July (within a month of the summer solstice, while surface waters are still heating and stratifying). Organic biomass associated with the blooms is usually low. This was especially well shown in the N. Atlantic coccolithophore bloom of 1991 (Fernández et al. 1993; Holligan et al. 1993). Even in non-bloom situations, the calcification:photosynthesis ratio peaks at 15% at chlorophyll levels $< 0.5 \mu\text{g L}^{-1}$ (Graziano et al. 2000). Moreover, calcification associated with the ephemeral blooms, as spectacular as they may be in satellite images, is of lesser significance globally due to their short 2-3 week duration (Balch et al. 1992; Graziano et al. 2000). Non-bloom calcification usually is between 1-3% of photosynthetic rates (Graziano et al. 2000; Marañón and González 1997), which, extended over time

and space scales of the world ocean, likely accounts for more carbon fixation into CaCO_3 .

Anatomy of a coccolithophore bloom

Many coccolithophore observations have been made in a Gulf of Maine phytoplankton sampling program, now in its 5th year, in which samples are taken from a ferry that travels between Yarmouth, Nova Scotia, Canada, and Portland, Maine, USA. A complete description is given in Balch et al. (2002). While most *E. huxleyi* observations have been made during non-bloom situations, in June 2000, a small coccolithophore bloom occurred along the ferry track that offered an ideal opportunity to sample and compare ship and satellite results (Fig. 5). The horse-shoe shaped bloom occurred at a frontal boundary (Fig. 6A), wrapped around the Jordan Basin within the Gulf of Maine, and the surface coccoliths were advected offshore, around the northern flank of Georges Bank. The feature was associated with strong backscattering peaks (Fig. 6B&C), and was associated with high water-leaving radiance values (as measured either from the ship's bow or from SeaWiFS (Fig. 6D)). Chlorophyll concentrations (estimated from ship and satellite) showed an offset of $0.25\mu\text{g Chl a L}^{-1}$, but were well-correlated nonetheless (Fig. 6E and I). Inherent optical properties (IOPs) of total scattering, absorption and attenuation showed well-defined peaks associated with the bloom. The absorption, scattering and attenuation of the dissolved material of $<0.2\mu\text{m}$ (colored dissolved organic matter; cDOM) showed the biggest increases in the Eastern Maine Coastal Current, on the western side of the transect near Portland (outside of the coccolithophore bloom). Nonetheless, careful inspection of Fig. 6G shows subtle increases in cDOM scattering in the coccolithophore bloom. This has never been reported before; it could have resulted from release of cDOM during grazing or viral infection of the coccolithophores. The size distribution of the algal community demonstrated good reproducibility for consecutive days (Fig. 7); the most negative slopes of the particle size distribution were associated with small diatoms, just east of the coccolithophore bloom, centered between $67.0\text{-}67.3^\circ\text{W}$. The region of diatoms within the eastern coccolithophorid patch was associated with a slight depression in the 550nm normalized water-leaving radiance (Fig. 6D).

Assembling all of the Gulf of Maine ferry data from 2000, it is apparent that the bloom occurred in a highly restricted part of the Gulf of Maine (along the Jordan Basin Frontal boundary), and was most concentrated near the end of June and early July. A 3-dimensional plot of total coccolith concentration versus daylength and water density (in sigma-theta units) illustrates exactly how narrow the space-time constraints were for this *E. huxleyi* bloom (Fig. 8). For example, peak coccolith concentrations were associated with day lengths approaching 16h (at the summer solstice), and moderate densities were located between low salinity, low density coastal waters and higher salinity, higher temperature Jordan Basin water (suggesting moderately stratified surface water at the frontal boundaries).

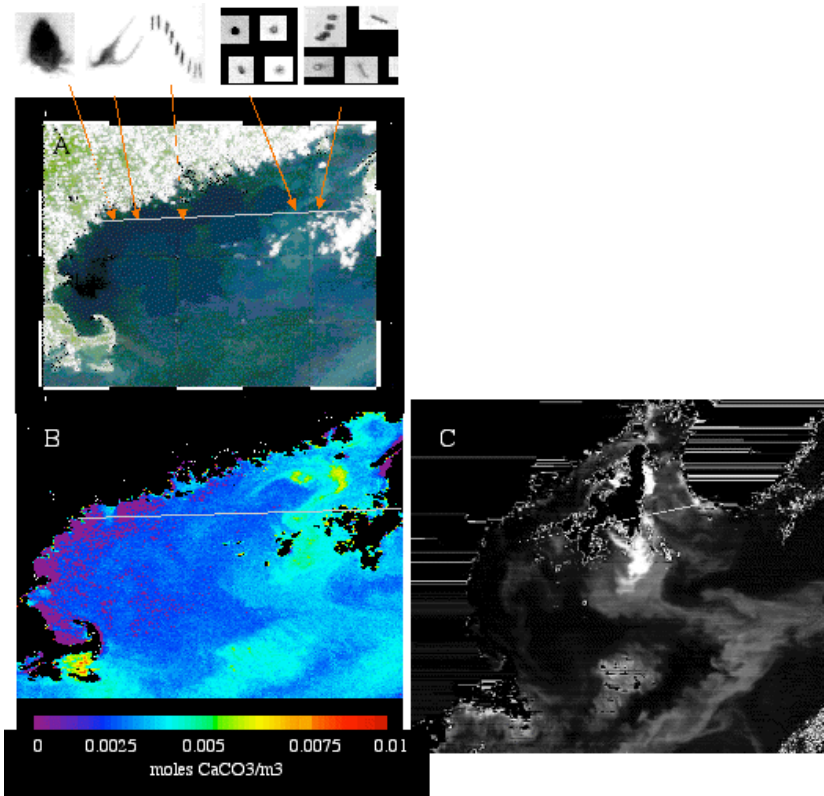


Fig. 5- A) True color image from 20 June, 2000, showing coccolithophore bloom region of high reflectance. Ferry track is shown with grey line in all panels. Dominant cells observed by FlowCam (a flow-through microscope) shown along top: (left to right- *Mesodinium* protozoa, *Ceratium* sp. (dinoflagellate), diatoms from coastal filament, coccolithophores, diatoms from Scotia Shelf. B) SeaWiFS image of CaCO_3 in Gulf of Maine (20 June, 2000) processed using Gordon et al. (2001) three-band algorithm. C) MODIS image of PIC concentration in Gulf of Maine from June 20, 2000. Note advection of coccoliths around northern flank of Georges Bank, with fine-scale eddy structure along the frontal boundary. Scale- White = 3×10^{-3} moles PIC m^{-3} ; light grey = 2×10^{-3} moles PIC m^{-3} ; dark grey = 0.75×10^{-3} moles PIC m^{-3} ; black = $0-0.1 \times 10^{-3}$ moles PIC m^{-3} .

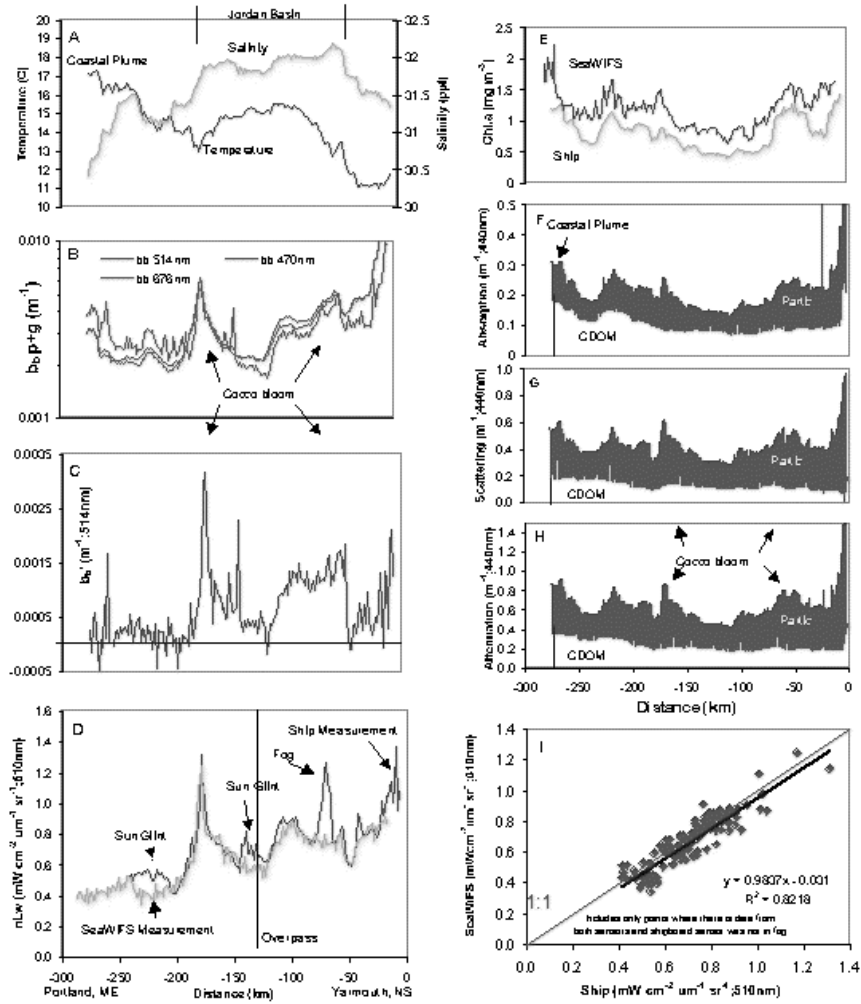


Fig. 6. Semi-continuous data taken from July 2, 2000 transect through Gulf of Maine coccolithophore bloom during its peak. Distance from Yarmouth, NS is on the X axis for panels A-H. A) Surface temperature and salinity. The eastern Maine coastal current and Jordan Basin water are indicated. B) Backscattering measured by the Wyatt light scattering photometer (514nm; based on 15 point volume scattering functions) and Hydrosat II (470 and 676nm; based on volume scattering at one angle). Water values have been subtracted, thus b_b values are from particulate and dissolved material (Balch et al. 1999). It can be seen that the Wyatt data show higher frequency variability than the HSII, which is due to the smaller viewed volume (9ml vs 20L). Moreover, both instruments clearly show similar trends, but their relative values vary, possibly due to changing shape of the volume scattering function (which is not taken into consideration with the HSII, but is with the Wyatt). The coccolithophore bloom is plainly visible in the backscattering on either side of the stratified Jordan Basin (60 and 170 km). C) Acid-labile backscattering at 514nm (b_b' ; measured with the Wyatt instrument), due to coccolith CaCO_3 . Values in coastal current are not significantly different from zero (FlowCAM showed the algal assemblage consisted of diatoms and dinoflagellates, with few coccolithophores). The ship moves 1.2 km during each 4 minute acidification cycle. Occasional negative b_b' values can result if phytoplankton b_b values *increase* (due to horizontal variability) during an acidification cycle (whereas b_b values should *decrease* due to CaCO_3 dissolution). In the coccolithophore bloom, calcite b_b' represented ~50% of the total backscattering at 514nm (compare with panel C). D) Satlantic radiometer data for normalized water-leaving radiance (nLw) compared with SeaWiFS values. At 60km, the ship passed through a fog bank, causing higher nLw values. Significantly increased nLw in the coccolithophore bloom was evident. E) Fluorescence- and SeaWiFS-derived (OC-4 model; (O'Reilly et al. 1998)) chlorophyll concentrations). One can see that the OC4 algorithm generally overestimates chlorophyll by $\sim 0.25 \mu\text{g l}^{-1}$ in the Gulf of Maine. F, G, H) IOP data on absorption, scattering, and attenuation taken with an ac-9 absorption and attenuation meter. Data shown here have had pure water values subtracted. The gray region represents particle IOPs (all particles $\geq 0.2 \mu\text{m}$ filtered), and the white region below represents the cDOM IOPs (water filtered through $0.2 \mu\text{m}$ poresize filters). One can see the increased cDOM absorption, scattering, and attenuation in the Eastern Maine coastal current. Also apparent in Jordan Basin is that 1/2 of the absorption, and 1/3 of the scattering is from cDOM. Scattering and absorption peaks were clearly evident in the coccolithophore bloom. I) SeaWiFS vs. ship-measured nLw 510 nm for data inside and outside coccolithophore bloom. Least-squares fit to the data has a slope that is not significantly different from 1.0.

It could be fortuitous that coccolithophore blooms generally happen close to the summer solstice for their respective hemisphere (i.e. due to the correct physical conditions of temperature and stratification). This seems unlikely, however. Cultures of *E. huxleyi*, in which other physical conditions are held constant, are day length saturated under 12-16h of light per 24h day (Paasche 2001). Indeed, our own culture studies have used a 14:10 light: dark cycle due to better growth of the clones (Balch et al. 1993).

The above re-parameterization of the *E. huxleyi* bloom to density and day length is, however, consistent with Margalef's Mandala (Margalef 1979) and it provides the possibility of extending it to include seasonal phytoplankton growth

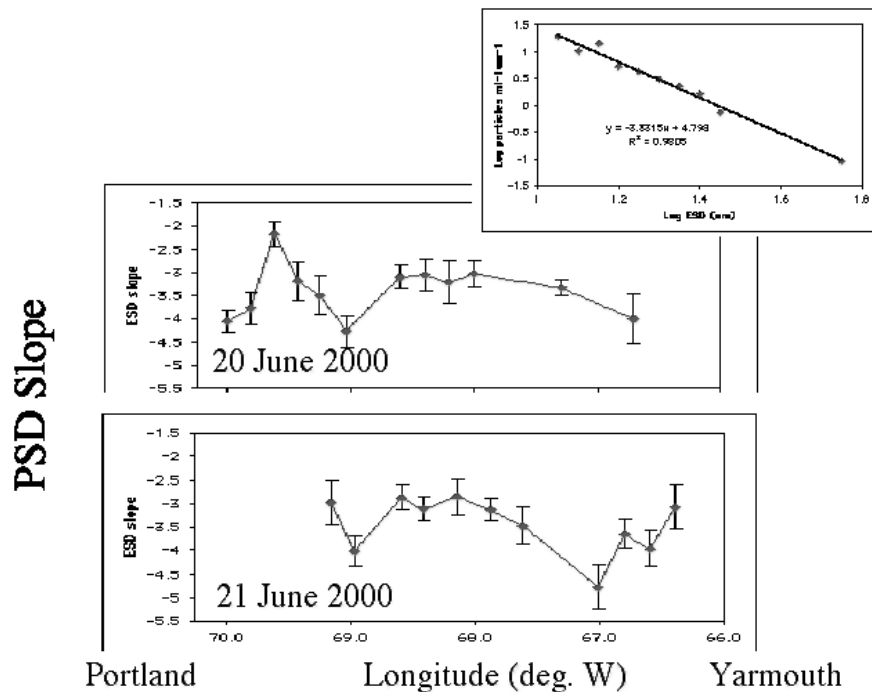


Fig. 7. Slopes of size distribution functions for each half-hour segment of Gulf of Maine ferry crossing as measured with Flow-Cam. Measurements were made on two consecutive days, 20 and 21 June 2000. Slopes were normalized to the bin size, according to Gin et al.(1999). Inset shows an example of a typical 1/2 hour Flow-Cam sample (sample from 6/20/00, 1146-1215h EDT) from which the slope and error limits on the slope are calculated.

preferences. Indeed, the striking association of the Gulf of Maine coccolithophore bloom to moderate surface density water provides indirect confirmation of its stability preference. (Note, we show elsewhere (Balch et al. 2002) that the density of surface water in the Gulf of Maine is well correlated to the vertical temperature gradient in the top 50m. Thus, the density axis in Fig. 8 is really indicative of vertical stratification). It could be argued that coccolithophore blooms occur in regions and times of moderate turbulence (and associated nutrient conditions).

Moreover, it is well-known from culturing studies of phytoplankton (not just coccolithophores) that, all other things being equal, phytoplankton growth rates respond to day length. There are clear examples of species which, given sufficiently high light intensities (e.g. *Ditylum brightwelli*), can grow close to their maximum growth rate with a 10h day (Eppley 1977; Paasche 1968). Moreover, the period of the spring diatom bloom occurs during March and April in the North Atlantic, with day lengths of about 10-12h. Laboratory and field results suggest

that diatoms are, at least, capable of exploiting these relatively short day lengths with high growth rates. Observations on day length preferences of dinoflagellates are rare. Brand and Guillard (1981) demonstrated that certain oceanic dinoflagellate species either required, or were favored by, a dark period. For dinoflagellate culturing, Guillard and Keller (1984) commented that, “light-dark cycles of 16-8, 14-10 and 12-12 hr. are commonly used”. Nonetheless, there are several observations of temperate dinoflagellate red-tides favoring longer day lengths (Nielsen 1992; Yentsch et al. 1975). For coccolithophores, experiments with *E. huxleyi* demonstrated that it had maximal growth rates at daylengths >16h (Paasche 1967), consistent with Fig. 8. Given these observations of daylength effects on phytoplankton growth, as a conceptual extension of Margalef’s Mandala, it seems reasonable that the two-dimensional mandala could be given a third axis of daylength (Fig. 9), as a way to a) better include coccolithophore blooms (Fig. 8) and b) provide differentiation for other species not yet included which likely will have their own day length preferences (e.g. cyanophytes, cryptophytes, prochlorophytes and the wealth of other picoplankton species). Day length could be considered one of several proximate (i.e., mechanistic) factors determining phytoplankton succession, *sensu* Guillard and Kilham (1977). Nonetheless, day length cues for growth would be subject to strong evolutionary selective pressures since changes in day length would help an organism unambiguously identify specific seasons (with

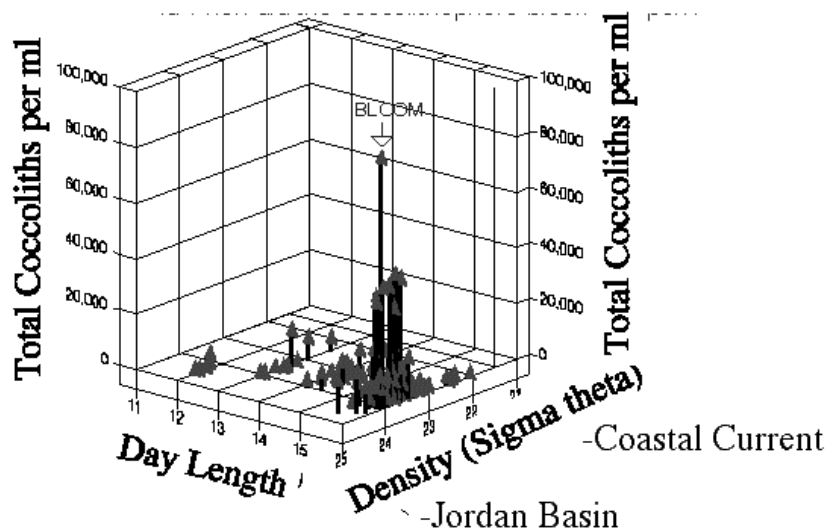


Fig. 8. Three-dimensional plot of total coccolith concentration versus daylength (in hours) and seawater density. This Gulf of Maine coccolithophore bloom reached its maximum coccolith density on 21 June 2000, when daylength approached 16h.

associated physical and chemical conditions). In emphasizing the potential importance of day length on phytoplankton community succession, the reader should not overlook the potential importance of grazing and its mechanistic controls on succession and bloom formation.

Use of optics to assess coccolithophore abundance

A major advantage in studying coccolithophores is the strong light scattering properties of their coccoliths. Calcium carbonate shows negligible absorption, but significant backscattering, of visible light (Balch et al. 1991). Thus, remote sensing can be used in ways not possible for other algal classes: knowing something about the physiological ecology of these organisms, plus their high visible-band reflectance, has allowed almost unambiguous identification of blooms from space.

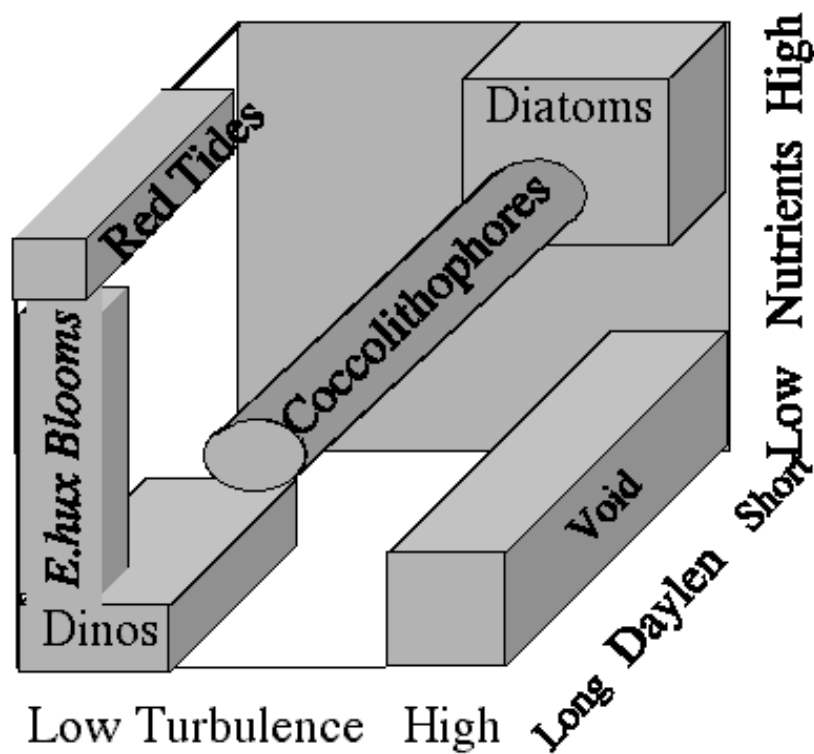


Fig. 9. Three-dimensional phytoplankton mandala in which a daylength axis has been added to Margalef's original two-dimensional mandala of nutrients and turbulence (Margalef 1979). Also coccolithophore blooms have been added.

There are some important exceptions, however, that can cause ambiguities in the optical interpretation of coccolithophore features. First, the light scattering is mostly due to the calcite coccoliths, whether or not they are attached to a coccosphere. High blue-green reflectance does not necessarily indicate high coccolithophore organic biomass. In fact, the term “bloom” is a misnomer for coccolithophores given that organic biomass is usually lower than in blooms of other algal species. It also has been shown that the light scattering properties of a coccolithophore suspension will be different depending on the ratio of loose coccoliths and plated cells (Balch et al. 1991; Voss et al. 1998). Thus, while plated coccolithophores have strong unique optical signatures, “naked coccolithophores” can be found in the sea and are not easily distinguished from other algal functional groups by remote sensing.

Another important issue for the optical characterization of coccolithophores is that coccoliths from different coccolithophore species will not scatter light to the same degree. It can be easily shown using calcite spheres, that the mass-specific scattering coefficient for calcite will be much lower for large calcite particles than small (Balch et al. 1996a). In nature, this means that foraminifera or pteropods will scatter light orders of magnitude less than the same mass of *E. huxleyi* coccoliths. Interestingly, the diameter of *E. huxleyi* coccoliths ($\sim 2\mu\text{m}$) optimizes their potential for scattering blue-green light (which also has fascinating evolutionary implications!). The remote sensing ramifications of this observation are that, on the one hand, it prevents mis-classification of foraminifera or pteropod suspensions as coccolithophore blooms when using remote sensing (because foraminifera or pteropods are typically much less abundant and scatter so little light per particle). On the other hand, the other ramification is that the mass-specific backscattering coefficient for calcite is not constant for the various species of coccolithophores (Balch et al. 1999) due to differences in coccolith morphology and degree of platedness. This likely sets the lower limit for the accuracy of any remote sensing calcite algorithm.

With the above caveats in mind, several remote sensing approaches have been applied to the study of coccolithophores. The Coastal Zone Color Scanner (CZCS) was used early-on for coccolithophore bloom observations, and differences were noted in the remote sensing reflectance spectra of coccolithophorids compared to other algal assemblages (Holligan et al. 1983). The Advanced Very High Resolution Radiometer (AVHRR) placed on various NOAA satellite platforms offered valuable information on coccolithophores, especially after the demise of CZCS. The AVHRR approach was to use the broad-band, but low sensitivity, channel 1 and correct it for clouds by subtracting the infra-red channel 2 (Groom and Holligan 1987). The approach allowed definition of bloom boundaries, but was not highly quantitative in terms of the amount of PIC or coccolith abundance, due to inaccuracies in the radiances. Nonetheless, the AVHRR approach allowed important documentation of blooms after the demise of CZCS and before the launch of the follow-on Ocean Color Thermal Sensor (OCTS) and Sea Wide Field-of-view Sensor (SeaWiFS).

Another approach, used mostly with SeaWiFS, was to generate coccolith flags, (i.e. regions within images with a high probability of being dominated by

coccolithophores). These flags have been invaluable for indicating regions where the chlorophyll algorithm would likely fail (Brown and Yoder 1994). Ackleson et al. (1994) also derived a technique for relating suspended calcite to radiance, based on Gulf of Maine data. Gordon et al. (1988) derived a quantitative, two-band algorithm for deriving the concentration of PIC, based on absolute values of 440 and 550nm water-leaving radiance, not radiance ratios. Their algorithm required, as input, the calcite-specific backscattering coefficient for *E. huxleyi* (Balch et al. 1999; Balch et al. 1996a; Balch et al. 1996b). The two-band algorithm iteratively solved for calcite concentration and chlorophyll and is currently being implemented by the Moderate Resolution Imaging Spectroradiometer (MODIS) sensor aboard NASA's Terra and Aqua satellite platforms (Esaias et al. 1998). A three-band calcite algorithm has also been derived, based on red and near infra-red bands (Gordon et al. 2001). The benefit of this latter algorithm is that it is not subject to absorption effects of chlorophyll and colored dissolved organic matter. This algorithm currently is being implemented with SeaWiFS data.

The two-band PIC algorithm of Gordon et al. (1988) has been validated, mostly using our data from the Gulf of Maine. Results suggest that the maximum RMS error of the algorithm is $\pm 17\mu\text{g PIC L}^{-1}$. This is about 5-10% of the PIC concentrations observed in a dense coccolithophore bloom but still greater than most PIC concentrations in non-bloom situations. One of the reasons for this error value is the vast array of PIC particles in the sea (e.g., the error analysis includes regions of suspended calcite sediments). For example, areas over Georges Bank frequently show high PIC concentrations but this likely is because the algorithm is "fooled" by high suspended sediments (in this case, sands). Nonetheless, in regions where there are no high concentrations of suspended sediments or other minerals, and the range in size of the PIC particles is fairly uniform, the precision of the two-band algorithm is $\sim 3\text{-}5\mu\text{g PIC L}^{-1}$, within the range of ambient PIC concentrations (details to be published separately). Moreover, by time and space binning of satellite PIC data, the standard error of the remote PIC estimates can be reduced sufficiently to allow PIC determination in the oligotrophic central oceans.

The first global views of surface PIC are being produced by SeaWiFS and MODIS and the results are striking (Fig. 10). Seasonal images clearly illustrate the importance of daylength on the appearance of high PIC concentrations (as mentioned earlier). That is, PIC concentrations in northern and southern hemisphere peak close to the respective summer solstice. Nowhere is this more obvious than in the North Atlantic and Argentine Continental Shelf regions. As described earlier, both are both regions of known coccolithophore blooms (Holligan et al. 1993). Another region that shows enhanced PIC concentrations is the Polar Frontal region of the Southern Ocean during the Austral summer. This is not an area known for coccolithophore blooms, and these results must be interpreted cautiously until more sea-truth data are available. This cautionary note is especially relevant considering that the Polar Front region is better known for diatom populations (Brzezinski et al. 2001) and, if biogenic silica is in high enough concentra-

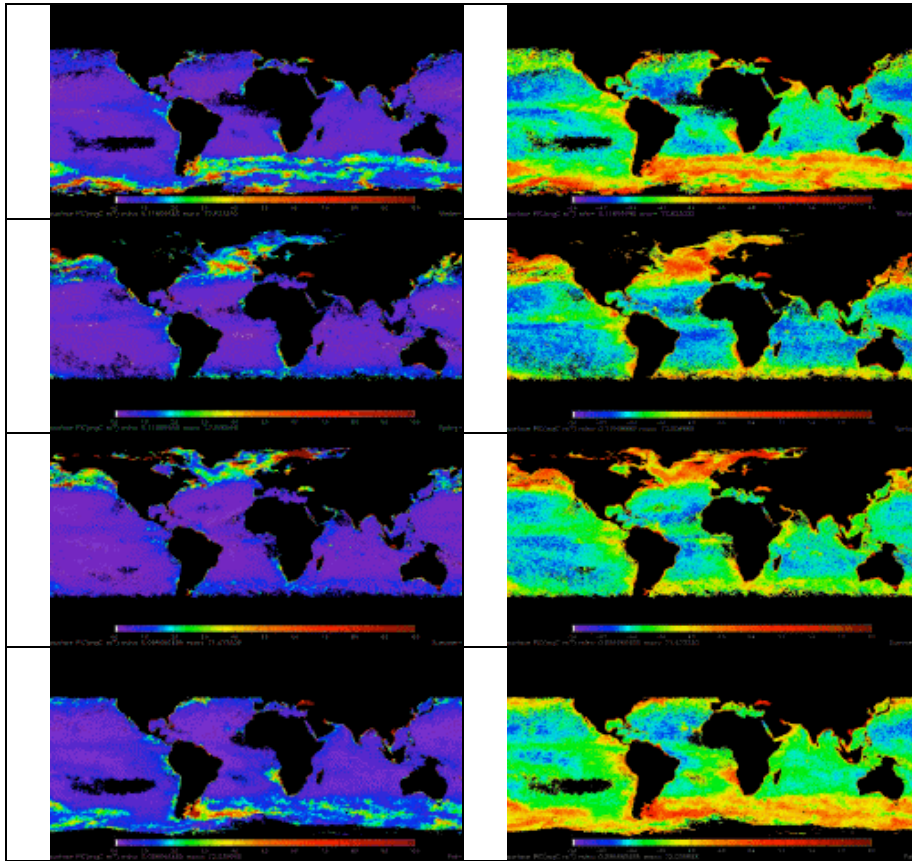


Fig. 10. Global views of PIC concentration taken by MODIS-Terra. Images were produced using Version 4 software, by performing averages of monthly mean images. Color scales on left-hand plots are linear, ranging from 0 (indigo) to 10 mg PIC m⁻³ (red), those on right-hand plots are logarithmic scales, with the following color scale in units of mg PIC m⁻³: 0.1=indigo, 1=green, 10=orange, 100=red. Seasonal periods are as follows: A & B) January through March, C & D) April to June, E & F) July to September, and G & H) October to December. PIC concentration was calculated using the two-band PIC algorithm based on Gordon et al. (1988).

tion, its backscattering might be confused with that of calcite. Nonetheless, the two-band algorithm was derived originally based on the light scattering properties of mixed phytoplankton assemblages, including diatoms. Thus, it should compensate for diatom scattering, as long as that scattering is associated with living cells, not resuspended frustules (containing no chlorophyll).

Can large-scale PIC distributions be related to Margalef's Mandala?

Given global maps of coccolithophore PIC, it is tempting to conclude that regions of high PIC are regions of high coccolithophore abundance (and to use carbon and cell abundance interchangeably within Margalef's Mandala). This interpretation is dangerous, however. For example, in the Arabian Sea, the highest coccolithophorid abundance was during the intermonsoon period, yet the highest calcification rates were during the Monsoon, the most productive period (Balch et al. 2000; Balch et al. 2001). In the Gulf of Maine, the highest calcification rates were not necessarily in regions with the most suspended PIC but often where overall primary production was greatest. In nonbloom situations, the typical calcification rate by the entire phytoplankton assemblage is between 0.1-30 g C gChl d⁻¹ (low, when compared to typical assimilation ratios for phytoplankton of 20-200 gC gChl d⁻¹ in the Gulf of Maine). The result is that calcification/photosynthesis ratios are not constant and, not surprisingly, vary from 0.1% to values >30%.

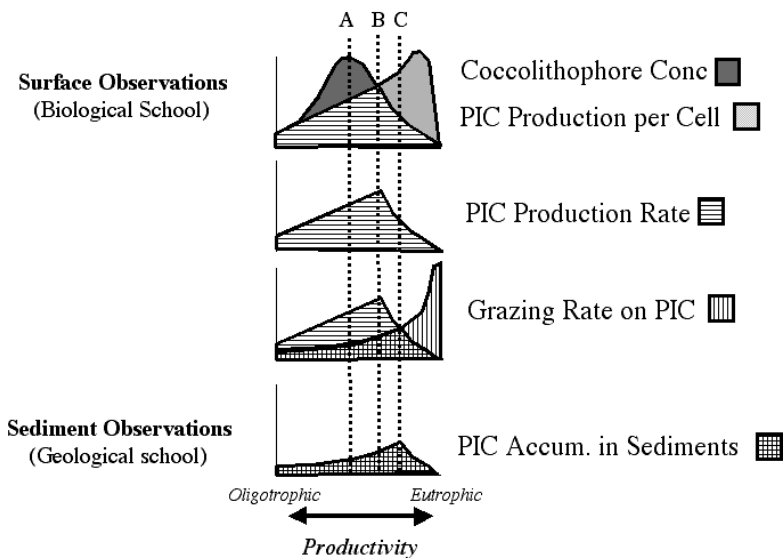


Fig. 11. Conceptual model for how coccolithophores can be most abundant in mesotrophic surface waters (“biological school”), yet they accumulate fastest in sediments underlying more eutrophic regions (“geological school”). Coccolithophore abundance has been shown along a gradient of productivity. Coccolithophore abundance, as suggested from the Margalef mandala, should peak in mesotrophic regions (line A). The product of the two curves for coccolithophore concentration and the calcification per cell (see Fig. 4), represents the total PIC production rate (second plot down). The curve in the PIC production rate (line B) is biased towards the higher production regions. Multiplying the PIC production curve by a variable PIC grazing rate (which is even more biased towards higher production regions) yields a PIC accumulation rate in the sediments that is highly biased towards high productivity zones (line C). Note, no aspects of carbonate preservation/dissolution are incorporated into this simplified view, only aspects of surface PIC production and grazing.

Studies of coccolithophore C fixation versus cell abundance have resulted in two fundamentally different schools of thought concerning coccolithophore distributions in space and time. The “geological school” associates sediments containing high numbers of coccolithophores with mixed overlying waters of high productivity. This is entirely consistent with our Arabian Sea and Equatorial Pacific carbon fixation observations. The Margalef Mandala, on the other hand, represents the “biological school”, in which coccolithophores are more likely found in moderately stratified waters, of moderate to low productivity. The many observations of healthy coccolithophore populations living on the stratified sides of frontal boundaries, next to well-mixed waters containing diatoms, supports the biological school. The only way both views can be considered internally consistent is if the calcification rate per cell is extremely variable (as shown in Fig. 4). This, combined with differences in grazing, can be incorporated into a conceptual model and used to explain the biological and geological views of coccolithophore abundance (Fig. 11). That is, the build-up of coccolithophore biomass in moderately stratified waters results from calcification occurring in an environment with 1) few grazers (which otherwise accelerate the downward flux of the PIC to the underlying sediments as ballasted fecal pellets) and 2) minimal vertical mixing. In highly productive situations, large grazers are more likely to be present, such that coccoliths and coccospheres would be rapidly transported to the sediments in fecal pellets and preserved in the geological record. Peak calcification would be observed in high productivity scenarios, as well, since populations are growing rapidly. In situations of moderate stratification, grazer abundance is more stochastic, such that there is a potential for a build-up of ungrazed coccolithophore PIC. Low grazing and high water column stability (low vertical mixing) mean that slow-sinking coccoliths can build-up to sufficient concentrations to cause turbid “blooms”. One important caution, however, is that grazing can also be associated with increased PIC dissolution (Harris 1994; Milliman et al. 1999); unfortunately, insufficient data exist to incorporate this into the conceptual model. Nonetheless, this conceptual model illustrates why interpreting the Margalef Mandala in terms of carbon does not necessarily follow from a conceptual model based on only cell abundance. Future efforts to understand coccolithophore abundance in space and time (from biological to geological time scales) will require better knowledge of the PIC transfer functions between the water column and sediments.

Acknowledgements

Many individuals have helped in this work with data collection and interpretation over the years: David Drapeau, Bruce Bowler, Emily Booth, Dr. Joaquim Goes (all Bigelow Laboratory for Ocean Sciences), Amanda Ashe (Oregon State University), Dr. Howard Gordon, Dr. Ken Voss, Katherine Kilpatrick, Dr. Jennifer Fritz and Charlie Byrne (all University of Miami), Dr. Liza Graziano (Sea Education Association), Dr. Patrick Holligan (University of Southampton, U.K.),

Dr. Emilio Fernandez (University of Vigo, Spain), and Dr. Robert Vaillancourt (Lamont Doherty, Columbia University). This work resulted from the generous support of various agencies over the years: National Aeronautics and Space Administration (NAGW2426; NAS5-97268; NAS5-31363; NAG5-10622); Office of Naval Research (ONR N00014-91-J-1048, N00014-97-1-0034; N00014-98-1-0882; N00014-01-1-0042), National Science Foundation (OCE-9022227; OCE-9596167), and NOAA (NA56RM0258; 40-AA-NE-005996).

References

- Ackleson S, Balch WM, Holligan PM (1994) The response of water-leaving radiance to particulate calcite and pigment concentration: A model for Gulf of Maine coccolithophore blooms. *J Geophys Res* 99: 7483-7499
- Archer D, Aiken J, Balch WM, Barber R, Dunne J, Flament P, Gardner W, Garside C, Goyet C, Johnson E, Kirchman D, McPhaden M, Newton J, Peltzer E, Welling L, White J, Yoder J (1997) A Meeting Place of Great Ocean Currents: Shipboard Observations of a Convergent Front at 2° N in the Pacific. *Deep-Sea Res II* 44: 1827-1849
- Balch WM, Drapeau D, Fritz J (2000) Monsoonal forcing of calcification in the Arabian Sea. *Deep-Sea Res II* 47: 1301-1337
- Balch WM, Drapeau D, Fritz J, Bowler B, Nolan J (2001) Optical backscattering in the Arabian Sea-continuous underway measurements of particulate inorganic and organic carbon. *Deep Sea Research I* 48: 2423-2452
- Balch WM, Drapeau DT, Bowler BC, Booth ES, Goes JJ, Ashe A, Frye JM (2002) A multi-year record of hydrographic and bio-optical properties in the Gulf of Maine: I. Spatial and temporal variability. *J Mar Res* Submitted
- Balch WM, Drapeau DT, Cucci TL, Vaillancourt RD, Kilpatrick KA, Fritz JJ (1999) Optical backscattering by calcifying algae--Separating the contribution by particulate inorganic and organic carbon fractions. *J Geophys Res* 104: 1541-1558
- Balch WM, Holligan PM, Ackleson SG, Voss KJ (1991) Biological and optical properties of mesoscale coccolithophore blooms in the Gulf of Maine. *Limnol Oceanogr* 36: 629-643
- Balch WM, Holligan PM, Kilpatrick KA (1992) Calcification, photosynthesis and growth of the bloom-forming coccolithophore, *Emiliana huxleyi*. *Cont Shelf Res* 12: 1353-1374
- Balch WM, Kilpatrick K (1996a) Calcification rates in the equatorial Pacific along 140 °W. *Deep-Sea Res II* 43: 971-993
- Balch WM, Kilpatrick K, Holligan PM, Harbour D, Fernandez E (1996a) The 1991 coccolithophore bloom in the central north Atlantic. II. Relating optics to coccolith concentration. *Limnol Oceanogr* 41: 1684-1696
- Balch WM, Kilpatrick KA (1996b) Calcification rates in the equatorial Pacific along 140°W. *Deep Sea Research* 43: 971-993
- Balch WM, Kilpatrick KA, Holligan PM (1993) Coccolith formation and detachment by *Emiliana huxleyi* (Prymnesiophyceae). *J Phycol* 29: 566-575

- Balch WM, Kilpatrick KA, Holligan PM, Trees C (1996b) The 1991 coccolithophore bloom in the central north Atlantic. I. Optical properties and factors affecting their distribution. *Limnol Oceanogr* 41: 1669-1683
- Brand LE, Guillard RL (1981) The effects of continuous light and light intensity on the reproduction rates of twenty-two species of marine phytoplankton. *J Exp Mar Biol Ecol* 50: 119-132
- Broerse ATC, Tyrrell T, Young JR, Poulton AJ, Merico A, Balch WM (2002) The cause of bright waters in the Bering Sea in winter. 2002 Submitted to *Cont. and Shelf Research*. *Cont Shelf Res* Submitted
- Brown CW, Yoder JA (1994) Coccolithophorid blooms in the global ocean. *J Geophys Res* 99: 7467-7482
- Brzezinski MA, Nelson DM, Franck VM, Sigmon DE (2001) Silicon dynamics within an intense open-ocean diatom bloom in the Pacific sector of the Southern Ocean. *Deep Sea Research II* 48: 3997-4018
- Buitenhuis, Bleijswijk EJv, Bakker D, Veldhuis M (1996) Trends in inorganic and organic carbon in a bloom of *Emiliania huxleyi* in the North Sea. *Mar Ecol Prog Ser* 143
- Eppley RW (1977) The growth and culture of diatoms. In: Werner D (ed) *The biology of diatoms*. Blackwell Scientific Publications, London, pp 24-64
- Esaias WE, Abbott MR, Brown OW, Campbell JW, Carder KL, Clark DK, Evans RL, Hoge FE, Gordon HR, Balch WM, Letelier R, Minnett P (1998) An overview of MODIS Capabilities for Ocean Science Observations. *IEEE Transactions on Geoscience and Remote Sensing, EOS-AM Special Issue* 36: 1250-1265
- Fernández E, Boyd P, Holligan PM, Harbour DS (1993) Production of organic and inorganic carbon within a large scale coccolithophore bloom in the northeast Atlantic Ocean. *Mar Ecol Prog Ser* 97: 271-285
- García-Soto C, Fernández E, Pinigree RD, Harbour DS (1995) Evolution and structure of a shelf coccolithophore bloom in the western English Channel. *J Plankton Res* 17: 2011-2036
- Gin KYH, Chisholm SW, Olson RJ (1999) Seasonal and depth variation in microbial size spectra at the Bermuda Atlantic time series station. *Deep -Sea Research I* 46: 1221-1245
- Gordon HR, Boynton GC, Balch WM, Groom SB, Harbour DS, Smyth TJ (2001) Retrieval of coccolithophore calcite concentration from SeaWiFS imagery. *Geochemical Research Letters* 28: 1587-1590
- Gordon HR, Brown OB, Evans RH, Brown JW, Smith RC, Baker KS, Clark DK (1988) A semianalytic radiance model of ocean color. *J Geophys Res* 93: 10909-10924
- Graziano L, Balch W, Drapeau D, B.Bowler, Dunford S (2000) Organic and inorganic carbon production in the Gulf of Maine. *Cont Shelf Res* 20: 685-705
- Groom S, Holligan PM (1987) Remote sensing of coccolithophore blooms. *Adv Space Res* 7: 73-78
- Guillard RL, Keller M (1984) Culturing dinoflagellates. In: Spector DL (ed) *Dinoflagellates*. Academic Press, Inc., New York, NY, pp 391-442
- Guillard RL, Kilham P (1977) The ecology of marine planktonic diatoms. In: Werner D (ed) *The Biology of Diatoms*. Blackwell Scientific Publications, London, England, pp 373-469
- Harris RP (1994) Zooplankton grazing on the coccolithophore *Emiliania huxleyi* and its role in inorganic carbon flux. *Mar Biol* 119: 431-439

- Holligan PM, Fernandez E, Aiken J, Balch W, Boyd P, Burkill P, Finch M, Groom S, Malin G, Muller K, Purdie D, Robinson C, Trees C, Turner S, van der Wal P (1993) A biogeochemical study of the coccolithophore, *Emiliana huxleyi*, in the north Atlantic. *Global Biogeochem Cycles* 7: 879-900
- Holligan PM, Viollier M, Harbout DS, Camus P, Champagne-Philippe M (1983) Satellite and ship studies of coccolithophore production along a continental shelf edge. *Nature* 304: 339-342
- Marañón E, González N (1997) Primary production, calcification and macromolecular synthesis in a bloom of the coccolithophore *Emiliana huxleyi* in the North Sea. *Mar Ecol Prog Ser* 157: 61-77
- Margalef R (1979) Life-forms of phytoplankton as survival alternatives in an unstable environment. *Oceanol Acta* 1: 493-509
- Milliman J, Troy PJ, Balch W, Adams AK, Li Y-H, MacKenzie FT (1999) Biologically-mediated dissolution of calcium carbonate above the chemical lysocline? *Deep-Sea Res* 46: 1653-1669
- Napp JM, Hunt GLJ (2001) Anomalous conditions in the south-eastern Bering Sea 1997: linkages among climate, weather, ocean and biology. *Fish Oceanogr* 10: 61-68
- Nielsen MV (1992) Irradiance and daylength effects on growth and chemical composition of *Gyrodinium aureolum* Hulbert in culture. *J Plankton Res* 14: 811-820
- O'Reilly JE, Maritorena S, Mitchell BG, Siegel DA, Carder KL, Garver SA, Kahru M, McClain C (1998) Ocean color chlorophyll algorithms for SeaWiFS. *J Geophys Res* 103: 24937-24953
- Okada H, Honjo S (1973) The distribution of oceanic coccolithophorids in the Pacific. *Deep-Sea Res* 20: 355-374
- Okada H, Honjo S (1975) The distribution of coccolithophorids in marginal seas along the western Pacific Ocean and in the Red Sea. *Mar Biol* 31: 271-285
- Okada H, McIntyre A (1977) Modern coccolithophores of the Pacific and North Atlantic oceans. *Micropaleontology* 23: 1-55
- Okada H, McIntyre A (1979) Seasonal distribution of modern coccolithophores in the western North Atlantic Ocean. *Mar Biol* 54: 319-328
- Paasche E (1967) Marine plankton algae grown with light-dark cycles. I. *Coccolithus huxleyi*. *Physiol Plant* 20: 946-956
- Paasche E (1968) Marine plankton algae grown with light-dark cycles. II. *Ditylum brightwellii* and *Nitzschia turgidula*. *Physiol Plant* 21: 66-77
- Paasche E (2001) A review of the coccolithophorid *Emiliana huxleyi* (Prymnesiophyceae), with particular reference to growth, coccolith formation, and calcification-photosynthesis interactions. *Phycologia* 40: 503-529
- Reid F (1980) Coccolithophorids of the North Pacific Central Gyre with notes on their vertical and seasonal distribution. *Micropaleontology* 26: 151-176
- Van der Wal P, Kempers RS, Veldhuis MJW (1995) Production and downward flux of organic matter and calcite in a North Sea bloom of the coccolithophore *Emiliana huxleyi*. *Mar. Ecol. Prog. Ser. Mar Ecol Prog Ser* 126: 247-265
- Voss K, Balch WM, Kilpatrick KA (1998) Scattering and attenuation properties of *Emiliana huxleyi* cells and their detached coccoliths. *Limnol Oceanogr* 43: 870-876
- Yentsch CM, Cole EJ, Salvaggio MG (1975) Some of the growth characteristics of *Gonyaulax tamarensis* isolated from the Gulf of Maine, in LoCicero VR, ed., *The First International Conference on Toxic Dinoflagellate Blooms*: Boston, MA, Massachusetts Science and Technology Foundation, p. 163-180.

Yoder JA, Ackleson SG, Barber RT, Flament P, Balch WM (1994) A line in the sea. *Nature* 371: 689-692

Young JR (1994) Functions of coccoliths. In: Winter A, Siesser WG (eds) *Coccolithophores*. Cambridge University Press, Cambridge, U.K., pp 63-82